

Ethylidyne Tricobalt Nonacarbonyl: Infrared, FT-Raman, and Inelastic Neutron Scattering Spectra

Stewart F. Parker*

ISIS Facility, Rutherford Appleton Laboratory, Chilton, Didcot, Oxon OX11 0QX, UK

Nicholas A. Marsh, Laure M. Camus, Michael K. Whittlesey,[†] and Upali A. Jayasooriya

School of Chemical Sciences, University of East Anglia, Norwich NR4 7TJ, UK.

Gordon J. Kearley

Interfacility Reactor Institute, Delft University of Technology, Mekelweg 15, 2629 JB Delft, The Netherlands

Received: December 31, 2001; In Final Form: April 1, 2002

The complex ethylidyne tricobalt nonacarbonyl is used as a model compound for ethylidyne chemisorbed on metal surfaces. In the present work, we have used the combination of infrared, FT-Raman and inelastic neutron scattering spectroscopies to test and extend previous assignments. We have located the missing mode, the torsion about the $\text{Co}_3\text{C}-\text{CH}_3$ bond. This occurs at 208 cm^{-1} and is highly mixed with the $\text{Co}_3\text{C}-\text{CH}_3$ bending mode. DFT calculations confirm that the frequency is a property of the molecule and is not imposed by solid-state effects. Accordingly, we would expect it to occur on a metal surface close to the frequency found in the complex. The FT-Raman spectra also show all of the carbonyl stretching modes for the first time and these are assigned by comparison to the DFT calculations. This also illustrates the maturity of the ab initio DFT methods in the prediction of INS spectra of compounds containing heavy elements.

I. Introduction

Ethylidyne, $\text{CH}_3\text{C}\equiv$, is a common product of the reaction of C_2 -containing molecules and fragments on metal surfaces for both single crystal (particularly (111) surfaces)^{1–5} and oxide-supported catalysts.^{6,7} The complex ethylidyne tricobalt nonacarbonyl, $\text{CH}_3\text{CCo}_3(\text{CO})_9$, (see Figure 1 for the structure) has been extensively used as a model compound for this species. In fact, the first correct identification⁸ of ethylidyne on metal surfaces was based on the vibrational spectrum of this complex.⁹

The complex crystallizes in the triclinic space group $P\bar{1} \equiv C_i^1$ (number 2) with two molecules in the unit cell.¹⁰ While each molecule lies on a general (C_1) site, both molecules have approximate C_{3v} symmetry. A comprehensive infrared and Raman spectroscopic study⁹ of $\text{CH}_3\text{CCo}_3(\text{CO})_9$, including the CD_3 and CD_2H derivatives, assigned 11 of the 12 modes associated with the CH_3CCo_3 unit. The remaining mode, the methyl torsion, was located by a subsequent inelastic neutron scattering (INS) study¹¹ at 383 cm^{-1} . This latter work was also particularly noteworthy in that it was the first demonstration of the feasibility of direct refinement of the force constants (obtained from a normal coordinate analysis) to the INS profile.

However, a number of questions still remain. There was a marked difference between the frequencies determined by the optical methods and by INS. There was a disagreement concerning the order of the frequencies of the asymmetric Co–Co stretch and the $\text{CoC}-\text{CH}_3$ bend. It has also become apparent that 383 cm^{-1} is unusually high for a methyl torsion; typical values lie between 46 cm^{-1} , as found in toluene,¹² and 250 cm^{-1} ,

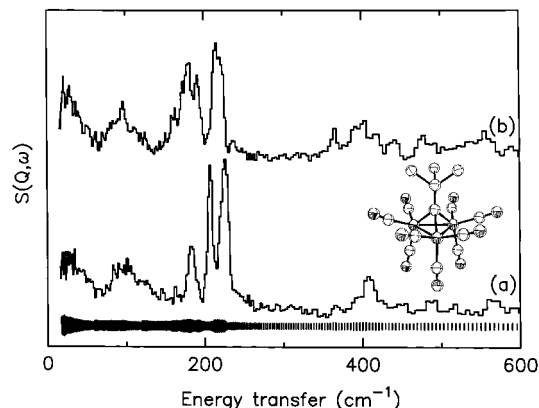


Figure 1. INS spectra of (a) ethylidyne tricobalt nonacarbonyl and (b) the mixture of isotopomers. The size of the error bars for both spectra are shown at the bottom of the figure. An ORTEP plot of the complex with the hydrogen atoms added is also shown.

as found in the *n*-alkanes.¹³ In addition, considerable advances in INS instrumentation and the understanding of the band-shaping processes have occurred. Together with the importance of the complex to catalysis, these questions have provided the motivation for remeasuring the vibrational spectra of ethylidyne tricobalt nonacarbonyl. To further substantiate the assignments and extend the analysis to the carbonyl modes, we have also used DFT to calculate the structure and vibrational spectra.

II. Experimental Section

$\text{CH}_3\text{CCo}_3(\text{CO})_9$ was prepared by a modification of a literature method:¹⁴ dicobalt octacarbonyl was reacted with ethyl dithioacetate¹⁵ in diethyl ether. An attempted preparation of the

* Fax: +44 1235 445720. E-mail: S.F.Parker@RL.AC.UK.

[†] Present address: Department of Chemistry, University of Bath, Bath BA2 7AY UK.

deuterated compound using ethyl dithioacetate- d_3 was only partially successful. Subsequent mass spectral analysis showed that the material was a mixture of isotopomers: CH_3 11.5%, CDH_2 35.2%, CD_2H 36.0%, CD_3 17.3%. The exchange probably occurred during the preparation of the intermediate dithioimidodiacetate- d_3 used to prepare the dithioacetate- d_3 .

The inelastic neutron scattering experiments were performed using the high-resolution broadband spectrometer (TFXA) at the ISIS pulsed spallation neutron source at the Rutherford Appleton Laboratory, Chilton, UK.¹⁶ TFXA offers high resolution, $\sim 2\%$ $\Delta E/E$ between 16 and 4000 cm^{-1} . The samples were held in aluminum sachets, cooled to 23 K, and the spectra were recorded for 12 h.

Raman spectra were recorded using a Fourier transform Raman spectrometer (Bruker IFS66 with an FRA 106 Raman module) with a nitrogen-cooled InGaAs detector and a 1064 nm excitation from a Nd:YAG laser. A 6-around-1 fiber-optic probe was coupled to the FT-Raman spectrometer as described elsewhere¹⁷ delivering 40 mW of laser power at the sample end. The spectra were simply recorded by immersing the probe head in the samples contained in glass vials. Spectra were recorded at room temperature and at 77 K at 2.0 cm^{-1} resolution using 400 scans each. For the measurements at 77 K, the sample vials were immersed in liquid nitrogen.

Mid-infrared, $4000\text{--}400\text{ cm}^{-1}$, spectra were recorded using a Mattson 5000 Fourier transform infrared (FTIR) spectrometer with a room-temperature deuterated triglycine sulfate (DTGS) detector at 1 cm^{-1} resolution. Spectra were recorded from KBr disks.

All energy calculations were carried out using the Density Function Theory package Dmol3¹⁸ on a single "isolated" molecule which allows an all-electron calculation to be performed. Localized basis sets were used, represented as a numerical tabulation: a DND double-numerical basis set with polarization functions was used. The radial extent of the integration mesh was 10 au, and the angular grid was adjusted to give numerical precision of 0.0001. In view of the large number of energy calculations to be made, we restricted ourselves to the Local Density Approximation LDA (Perdew–Wang). The vibrational spectra were calculated in the harmonic approximation using the finite displacement technique to obtain the dynamical matrix. Starting from given geometries, each of the atoms in the unit cell was displaced by 0.1 \AA in turn along the three Cartesian directions and a single-point calculation gives the Hellmann–Feynman forces on all the atoms, from which the force constants are obtained by dividing by the displacement. Positive and negative displacements were used in order to obtain more accurate central finite differences. The force constant matrix \mathbf{F} was transformed to mass-dependent coordinates by the \mathbf{G} matrix giving the dynamical matrix. Diagonalization of the dynamical matrix gives the vibrational eigenvalues and eigenvectors.

III. Results and Discussion

If the symmetry of the complex is assumed to be C_{3v} , then the 18 vibrations of the Co_3CCH_3 fragment may be classified as $5A_1 + A_2 + 6E$ and the 9 $\text{C}\equiv\text{O}$ stretching vibrations as $2A_1 + A_2 + 3E$. In C_1 symmetry, all symmetry is lost. Since on metal surfaces ethynylidyne usually has C_{3v} symmetry, we will use the C_{3v} symmetry labels and highlight where the approximation breaks down.

The infrared spectra of the complex and its isotopomers have been published previously,⁹ and our results are in good agreement with them. The INS and FT-Raman spectra of

ethynylidyne tricobalt nonacarbonyl for the hydrogenous compound and the mixture of isotopomers are shown in Figures 1–3. The INS spectrum of the hydrogenous compound is markedly superior to previous results: the resolution is much better and the energy transfer range is extended to both lower and higher wavenumber. The improvements in instrument performance mean that more modes are detected. The INS spectrum of the mixture of isotopomers has not been observed previously. The FT-Raman spectra show, for the first time, the modes of the ethynylidyne ligand in addition to the carbonyl and metal–metal modes. Table 1 lists the observed frequencies and their assignments.

The 77 K FT-Raman spectra, Figures 2 and 3, clearly show the C_1 symmetry of the complex. The E mode at 2925 cm^{-1} is split into two components, as would be expected for C_1 symmetry. This is not due to factor group splitting, since the space group is centrosymmetric; thus only one of the two factor group modes would be Raman active. The splitting provides a straightforward method for the assignment of the E modes (provided they appear in the Raman spectrum), as was also found for methyltrioxorhenium.¹⁹ Thus, the mode at 225 cm^{-1} is markedly asymmetric, and the band at 180 cm^{-1} at room temperature is clearly split at 77 K in agreement with the assignment to E modes. In contrast, the bands at 410 and 240 cm^{-1} are single peaks as expected for A_1 modes.

The frequencies for the C–H and C–D stretching and bending regions of the CH_3 , CH_2D , and CD_3 compounds are very close to those of Skinner et al.,⁹ and the assignments are the same. The 77 K FT-Raman spectrum, Figure 3, shows six bands in the C–H stretch region while only five are expected. Two of these are very close at 2889 and 2895 cm^{-1} , so they are both assigned to the symmetric stretch of the CH_2D isotopomer. The presence of two bands may reflect that the C–H bonds are not equivalent, since the true symmetry is C_1 . For the CHD_2 isotopomer, the modes are observed for the first time; see Table 1.

INS intensities depend on the amplitude of vibration and the incoherent scattering cross section of the atoms. Since the incoherent cross section of hydrogen is $\sim 80 \times 10^{-28}\text{ m}^2$ and those of deuterium, carbon, and cobalt are all less than $\sim 5 \times 10^{-28}\text{ m}^2$, the hydrogenic motions will dominate the INS spectrum. Further, the requirement is only for proton motion: modes that result in no change in the bond angles or distances associated with the hydrogen atom but result in proton motion (riding) will have INS intensity. The dependence on the cross section also results in no symmetry-based selection rules.

Inspection of the INS spectrum in the low-energy region ($<300\text{ cm}^{-1}$) shows intensity below 70 cm^{-1} that can be assigned to the external modes of the complex. A structured feature at 100 cm^{-1} , that by comparison to the FT-Raman spectrum, can be assigned to the $\text{OC}\text{--}\text{Co}\text{--}\text{CO}$ bending modes and the band at 182 cm^{-1} due to the asymmetric $\text{Co}\text{--}\text{Co}$ stretch. Two intense features occur at 208 and 224 cm^{-1} . In methyl compounds, e.g., methyltrioxorhenium,¹⁹ the most intense band in the INS spectrum is usually the methyl torsion. The observation of two strong bands in this region is evidence that the dynamics of this complex are unusual.

It is possible that two bands are observed because of factor group splitting; the absence of selection rules means that both components would appear in the INS spectrum. This is unlikely, since no other mode in the INS spectrum shows any indication of splitting. In addition, it would be expected that the two modes would be of equal intensity, rather than the 1:1.7 ratio (208:224) observed.

TABLE 1: Wavenumbers (cm⁻¹) of the Observed Bands and Their Assignments

CH ₃ CCO ₃ (CO) ₉			CH _(3-x) D _x CCO ₃ (CO) ₉ (x = 0-3)				assignment				
DFT (km mol ⁻¹)	IR (RT)	Raman (77 K)	INS (20 K)	IR (RT)	Raman (RT)	Raman (77 K)	INS (20 K)	H ₃	H ₂ D	HD ₂	D ₃
3004 (3)	2930 m	2927/292 0 m		2929 m	2930 vw	2926 w		$\nu_{as}CH_3$ E			
				2926 m	2915 vw	2920 w			$\nu_{as}CH_2$		
				2910 vw	2907 vw	2905 w			ν_sCH_2	νCH	
				2901 vw	2900 vw	2895 w/ 2889 w					
2923 (11)	2888 m 2840 w 2822 w 2780 w 2450 br	2880 s 2814 vw		2888 vw	2888 vw	2880 w		ν_sCH_3 A ₁ 2· $\delta_{as}CH_3$ 2· δ_sCH_3 $\delta_{as}CH_3 + \delta_sCH_3$ $\nu CO + \delta CoCO$			
				2199 vw						$\nu_{as}CD_2$	$\nu_{as}CD_3$
				2195 vw		2193 w			νCD		
				2188 vw							
				2167 vw		2163 w					ν_sCD_3
2145 (98)	2104 m ^b	2102 s			2100 s	2102 vs		νCO A ₁			
2100 (1948)	2052 vs ^b	2056 s			2054 m	2056 s		νCO E			
		2045 m			2042 m	2044 w					
2091 (1640)	2038 vs ^b	2033 s			2030 m	2032 s		νCO A ₁			
2066 (19)	2018 m ^b	2014 vs			2009 vs	2014 vs		νCO E			
2058 (2)		2006 sh/2001 vs		2001 vs	2000 vs	2006 sh/ 2001 vs		νCO E			
2048 (0)		1995 s				1995 s		νCO A ₂			
		1963 vw			1966 vw	1965 w		$\nu^{13}CO$			
1402 (6)	1420 m	1426 w	1433 w	1420 m	1425 w			$\delta_{as}CH_3$ E			
1353 (47)	1356 m	1356 w		1358 m	1357 vw	1355 w		δ_sCH_3 A ₁			
				1264 m	1267 vw	1261 w	1261 m			δCH	
				1182 m		1184 vw					νCC
1220 (38)	1163 m			1161 m		1162 w		νCC A ₁			$\delta_{as}CD_3$
				1029 w						δCD_2	δ_sCD_3
				1021 w							
				1007 m							
991 (51)	1004 s		1009 m					ρCH_3 E			
606 (175)	555 vs		565 w				976 w,br 556 w	$\nu_{as}Co\equiv CCH_3$ E			
579 (4)											
578 (72)	525 s	530 w	529 w					$\nu Co-CO$			
569 (75)	515 s							$\nu Co-CO$			
553 (24)	502 vs							$\delta Co-CO$			
547 (1)											
526 (8)		491 w	488 w			489 w					
515 (0)											
509(31)	470 s	480 w			479 vw	479 w	476 w	$\delta Co-CO$			
499 (0)											
488 (4)	435 w	440 w			437 m	439 w		$\delta Co-CO$			
473 (0)		423 w				422					
437 (2)											
432 (4)	401 m	410 s	408 m		404 mw	405 m	404 m	$\nu_sCo\equiv CCH_3$ A ₁			
417 (2)		392 w									
416 (4)											
						391 w			$\nu_sCo\equiv CCH_{(3-x)}D_x$		
380 (0)											
376 (0)			364 w				364 w				
259 (0)	235 vw	240 vs			233 s	240 vs		ν_sCo-CO A ₁			
230 (0)	221 vw	223 m/221 sh	224s		223 sh	223 sh		$\delta CoC-C$ H ₃ E			
					212 w	214 m		$\delta CoCCH_2D$			$\delta CoCCH_2D_2$
200 (0)			208 s				215 s	τCH_3 A ₂			
185 (0)	180 vw	186/180 s	182 m				193 s	$\nu_{as}Co-CO$ E	τCH_2D		
					177 m	181 m 175 sh	174 sh 162 m		$\nu_{as}Co-COCH_2D$		$\nu_{as}Co-CO$ CHD ₂
						142 m 121 s					τCHD_2
114 (0)		142 m 120 s 109 w	116 m		117 m	109 w		$\delta COCoC$ O			
106 (0)		102 s	100 m		98 s	102 s	96 m	$\delta COCoC$ O			
98 (0)		94 s				94 s					
93 (1)		82 m	84 m			81 m	84 m	$\delta COCoC$ O			
87 (0)		77 m			78 m	77 m					
85 (0)											
79 (0)											
65 (0)											
56 (0)											
32 (0)											
-14 (0)			28 m				28 m	c	c	c	c

^a Key: s = strong, m = medium, w = weak, v = very, br = broad, sh = shoulder. ^b As hexane solution, data from Bor.²³ ^c Lattice and acoustic modes.

The 224 cm⁻¹ band has been previously assigned to the CoC-CH₃ bending mode; thus the 208 cm⁻¹ is assigned as the torsion, in contrast to the earlier assignment at 383 cm⁻¹.¹¹

One of the advantages of INS spectroscopy is that it is

possible to use the intensities as constraints in a normal coordinate analysis. The program CLIMAX^{11,20} has been developed to carry-out such an analysis based on the Wilson-Decius-Cross²¹ method. As input, we have used the heavy atom

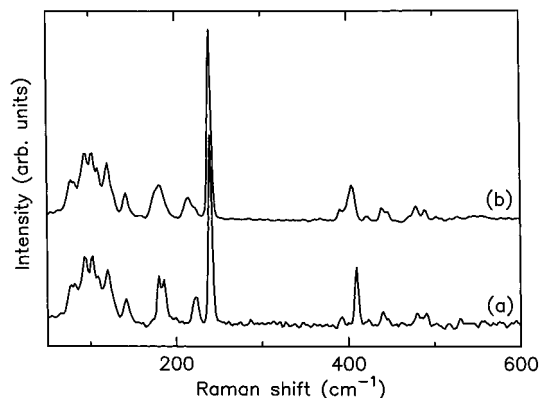


Figure 2. FT-Raman spectra at 77 K of (a) ethynylidyne tricobalt nonacarbonyl and (b) the mixture of isotopomers in the region 50–600 cm^{-1} .

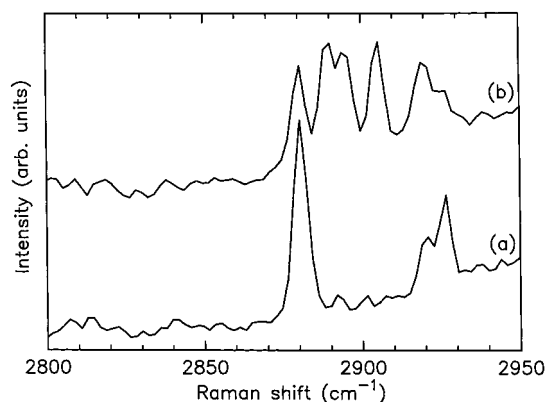


Figure 3. FT-Raman spectra at 77 K of (a) ethynylidyne tricobalt nonacarbonyl and (b) the mixture of isotopomers in the C–H stretching region. Relative to Figure 2, part a is scaled by $\times 3$ and part b by $\times 14$.

geometry determined by X-ray diffraction¹⁰ and the methyl group geometry determined from the infrared frequencies.²² If the torsion is assigned to the 224 cm^{-1} band (since it is the most intense) and the bend to the 208 cm^{-1} band, then we are unable to derive a force field that will reproduce even the observed frequencies. (This assignment is also incompatible with the 77 K FT-Raman data). With the torsion at 208 cm^{-1} and the bend at 224 cm^{-1} , using the force constants of Skinner et al.⁹ plus an additional one for the torsion, we obtain an excellent frequency fit. However, comparison of the observed, Figure 4a, and predicted INS intensities, Figure 4b, shows very poor agreement. This suggests that the torsion is mixed with another vibration and the total intensity is redistributed across the two modes.

Introduction of off-diagonal terms between the torsion and the CoC–CH₃ bending mode and between the torsion and the Co–Co stretch resulted in the excellent agreement shown in Figure 4c. This mixing is a direct consequence of (i) the C_1 symmetry of the molecule, since in C_{3v} symmetry there is no operation that couples the torsion with any other mode, and (ii) the small difference in energy that allows substantial mixing. Even partial deuteration shifts the torsion sufficiently to eliminate the mixing.

The force field can be used to predict the spectra of the isotopomers. The D₃ isotopomer can be neglected since the cross section is more than an order of magnitude smaller than that of the hydrogenous ones. Inspection of Figure 1b shows that there is only a very weak shoulder at 208 cm^{-1} so the contribution of the H₃ isotopomer can also be neglected. The mass spectrometric analysis indicated that there was approximately

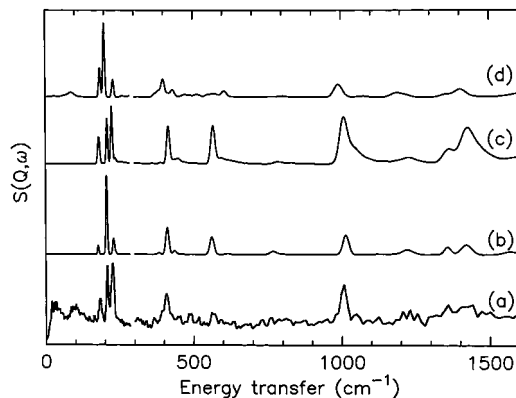


Figure 4. (a) Observed INS spectrum of ethynylidyne tricobalt nonacarbonyl in the 100–600 cm^{-1} region, (b) spectrum calculated using the force field of Skinner et al.,⁹ (c) spectrum as in part b but with an off-diagonal term between the torsion and the Co–Co stretch, and (d) spectrum as calculated by DFT. All spectra are $\times 2$ ordinate expanded in the 300–600 cm^{-1} region.

TABLE 2: Comparison of Average Structural Parameters for the Complex

distance (Å)	DFT	X-ray
Co–Co	2.428	2.467
Co–CCH ₃	1.885	1.90
Co ₃ C–CH ₃	1.467	1.53
C–H	1.108	1.099 ^a
Co–CO	1.785	1.80
CoC=O	1.149	1.10
angles (°)		
H–C–H	107.6	106.5 ^a
Co–Co–CCH ₃	49.9	49.4
Co–C=O	178.5	175.0

^a Calculated using the method described previously.²⁰

equally quantities of the H₂D and the HD₂ isotopomers. Curve-fitting the spectrum showed the presence of six peaks at 223, 215, 193, 182, 174, and 162 cm^{-1} . From the force field, these are assigned as (predicted values in brackets): 223 (224/220) $\delta\text{CoCCH}_2\text{D}$, 193 (187) $\tau\text{CH}_2\text{D}$, 174 (178/174) $\nu_{\text{as}}\text{Co–CoCHD}_2$ and 215 (217) δCoCCHD_2 , 182 (179/177) $\nu_{\text{as}}\text{Co–CoCHD}_2$, 162 (163) τCHD_2 . The excellent agreement is further confirmation of the correctness of the assignments.

To verify the assignments and to extend the analysis to include the carbonyl ligands, the structure and vibrational spectra of the complex were computed using DFT. The minimum energy structure has C_1 symmetry. A comparison of the structural parameters is given in Table 2, and it can be seen that the agreement is very good, particularly in view of the complexity of the molecule. As a further check, the INS spectrum was generated from the atomic displacements of the modes as described elsewhere²⁰ and is shown in Figure 4d. It can be seen that the agreement is good, although the intensities of the methyl torsion and the CoC–CH₃ bending mode are somewhat underestimated. However, in addition to the ethynylidyne modes, the broad hump of intensity at 100 cm^{-1} due to the OC–Co–CO bending modes is reproduced, as are the weak features around 500 cm^{-1} due to the Co–CO stretch and Co–C≡O bending modes. Inspection of the eigenvectors of the modes confirms the original assignment of the asymmetric Co–Co stretch and the CoC–CH₃ bend to the bands at 182 and 224 cm^{-1} , respectively.

Having shown that the DFT result gives a reasonable description of the dynamics, we can use it to assign the carbonyl modes. If C_{3v} symmetry is assumed for the fragment, then six

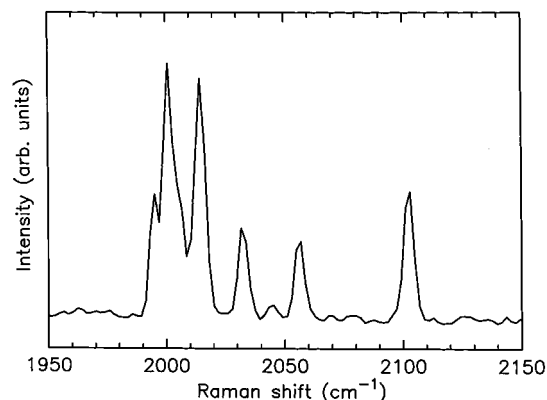


Figure 5. FT-Raman spectrum of the carbonyl region of the protonated complex at 77 K. (Unscaled relative to Figure 2).

TABLE 3: Comparison of Surface-Bound Ethyldiyne Frequencies with Those of Ethyldiyne Tricobalt Nonacarbonyl

mode	complex	Pt(111) ^{2,3}	Ni(111) ²²
$\nu_{as}CH_3$ E	2930	2950	2940
ν_sCH_3 A ₁	2888	2884	2883
$\delta_{as}CH_3$ E	1420	1420	1410
δ_sCH_3 A ₁	1356	1339	1336
ν_{CC} A ₁	1163	1124	1129
ρ_{CH_3} E	1004	980	1025
$\nu_{as}Co\equiv CCH_3$ E	555	600	457
$\nu_sCo\equiv CCH_3$ A ₁	401	430	362
ν_sCo-Co A ₁	242	160	
δ_{CoC-CH_3} E	224	310	
τ_{CH_3} A ₂	208		
$\nu_{as}Co-Co$ E	180		

$C\equiv O$ stretching modes ($2A_1 + A_2 + 3E$) are expected. The C_1 symmetry would formally lift all the degeneracies; however, since the infrared and FT-Raman spectra show only six bands (plus a ^{13}CO satellite), any splitting of the E modes must be less than the bandwidth. On the basis of the four modes visible in the infrared spectrum, the stretching modes have been previously assigned.²³ The room temperature Raman spectrum shows six strong modes, of which the band at 2000 cm^{-1} has a distinct shoulder. At 77 K, Figure 5, the bands sharpen and intensify; however, the band at 2045 cm^{-1} does not follow this pattern, so we assign it to an overtone or combination of the deformation modes in Fermi resonance with a fundamental. The shoulder is partially resolved at 1995 cm^{-1} , and a second shoulder appears at 2006 cm^{-1} . If the DFT frequencies are reduced by 50 cm^{-1} , then the frequencies closely match the observed infrared and Raman frequencies and the predicted infrared intensities follow the observed pattern. The DFT results show that the 2001 cm^{-1} band with the shoulder at 2006 cm^{-1} is the lowest E mode and the 1995 cm^{-1} mode is the A_2 mode. The six bands are assigned as given in Table 1, in agreement with the previous assignment.

The assignment of the $Co-CO$ stretch and $Co-C\equiv O$ bending modes is more difficult because many fewer modes are observed than are predicted. Since the observed pattern of intensities in the infrared spectrum is reproduced by the DFT results, we have assigned the spectra accordingly.

The interest in this complex arises from its use as a model compound for surface-bound ethyldiyne. In Table 3, we compare the frequencies for the complex with EELS and RAIRS data for ethyldiyne on metal single crystals.^{2,3,24} It confirms that the complex is a superb model for the modes that are due to C-H stretch and bend motions. For the lower energy modes, the

situation is less clear. Unsurprisingly, the $M-C$ stretch modes are metal-dependent, although the difference from those of the cluster is only on the order of 10%. The $Co_3\equiv C-CH_3$ bend is higher than that in the cluster; again this might be expected to be metal-dependent. The torsion has not yet been observed, although a recent study²⁴ concluded that it must lie below 260 cm^{-1} . The high frequency for the torsion found in the complex indicates that it is not due to solid-state effects; in toluene,¹² there is essentially free rotation in the gas phase and the solid state frequency is only 46 cm^{-1} . This conclusion is supported by the DFT results for the complex which are an isolated, i.e., gas-phase molecule calculation, which predicts it at 200 cm^{-1} . Since the torsion does not directly interact with the surface, it might be expected to be independent of the nature of the surface, exactly as the C-H stretch and bend modes are. Accordingly, we would expect it to occur on a metal surface close to the frequency found in the complex, 208 cm^{-1} .

IV. Conclusions

Ethyldiyne tricobalt nonacarbonyl has been the first and the most successful model compound in the identification of ethyldiyne groups on catalytically important surfaces. The powerful combination of modern DFT methods with the vibrational spectroscopic techniques of IR, Raman, and INS has resulted in a complete assignment of all the fundamental vibrations of this compound. The present investigation has thus clarified the doubts that existed in the literature regarding several of the assignments. Particularly, the $Co_3\equiv C-CH_3$ bend is proven to be of higher frequency than the asymmetric $Co-Co$ stretch, and the methyl torsion is reliably assigned to a frequency at 208 cm^{-1} , rather than the 383 cm^{-1} previously reported. With the continuous progress that is being made with neutron scattering sources and instrumentation, application of inelastic neutron scattering techniques to real catalytic systems is becoming a reality. Vibrational normal modes with high-amplitude proton motion such as methyl torsions and rocking modes are likely to be the early candidates for INS characterization of catalytic species on surfaces. Therefore, the results presented here provide all the INS data for the identification of this most abundant surface species, ethyldiyne.

Acknowledgment. The Rutherford Appleton Laboratory is thanked for access to neutron beam facilities.

References and Notes

- (1) Kesmodel, L. L.; Gates, J. A. *Surf. Sci.* **1981**, *111*, L747.
- (2) Steininger, H.; Ibach, H.; Lehwald, S. *Surf. Sci.* **1982**, *117*, 685.
- (3) Chesters, M. A.; de la Cruz, C.; Gardner, P.; McCash, E. M.; Prentice, J. D.; Sheppard, N. *J. Electron Spec. Relat. Phenom.* **1990**, *54*, 739.
- (4) Ransley, I. A.; Ilharco, L. M.; Bateman, J. E.; Sakakini, B. H.; Vickerman, J. C.; Chesters, M. A. *Surf. Sci.* **1993**, *298*, 187.
- (5) Fan, J.; Trenary, M. *Langmuir* **1994**, *10*, 3649.
- (6) Beebe, T. P.; Yates, J. T., Jr. *J. Phys. Chem.* **1987**, *91*, 254.
- (7) Mohsin, S. B.; Trenary, M.; Robota, H. J. *J. Phys. Chem.* **1991**, *95*, 6657.
- (8) Chesters, M. A.; Sheppard, N. *Chem. Brit.* **1981**, *17*, 521.
- (9) Skinner, P.; Howard, M. L.; Oxtton, I. A.; Kettle, S. F. A.; Powell, D. B.; Sheppard, N. *J. Chem. Soc., Faraday Trans. 2* **1981**, *77*, 1203.
- (10) Sutton, P. W.; Dahl, L. F. *J. Am. Chem. Soc.* **1967**, *89*, 261.
- (11) Kearley, G. J. *J. Chem. Soc., Faraday Trans. 2* **1986**, *82*, 41.
- (12) Cavagnat, D.; Lascombe, J.; Lassegues, J. C.; Horswill, A. J.; Heidemann, A.; Suck, J. B. *J. Physique* **1984**, *45*, 97.
- (13) Braden, D. A.; Parker, S. F.; Tomkinson, J.; Hudson, B. S. *J. Chem. Phys.* **1999**, *111*, 429.
- (14) Patin, H.; Mignani, G.; van Hulle, M. T. *Tetrahedron Lett.* **1979**, 2441.

- (15) Marvel, C. S.; De Radzitsky, P.; Brader, J. J. *J. Am. Chem. Soc.* **1955**, *77*, 5997.
- (16) Penfold, J.; Tomkinson, J. *The ISIS Time Focused Crystal Spectrometer, TFXA*; RAL-86-019, 1986.
- (17) Sprunt, J. C.; Jayasooriya, U. A. *Appl. Spectrosc.* **1997**, *51*, 1410.
- (18) Delley, B. *J. Chem. Phys.* **1990**, *92*, 508.
- (19) Parker, S. F.; Herman, H. *Spec. Acta* **2000**, *56A*, 1123.
- (20) Kearley, G. J. *Nucl. Inst. Methods Phys. Res. A* **1995**, *354*, 53.
- (21) Wilson, E. B., Jr.; Decius, J. C.; Cross, P. C. *Molecular Vibrations*; Dover: New York, 1955.
- (22) Parker, S. F.; Jayasooriya, U. A. *Surf. Sci.* **1996**, *368*, 275.
- (23) Bor, G. *Inorg. Chim. Acta* **1969**, *3*, 56.
- (24) Bürgi, T.; Trautman, T. R.; Haug, K. L.; Utz, A. L.; Ceyer, S. T. *J. Phys. Chem.* **1998**, *102*, 4952.